Dye-Sensitized SnO_2 Electrodes with Iodide and Pseudohalide Redox Mediators

Bryan V. Bergeron,[†] Andras Marton,[†] Gerko Oskam,[‡] and Gerald J. Meyer*[,†]
Department of Chemistry and Department of Materials Science and Engineering, The Johns Hopkins University, Baltimore, Maryland 21218, and Departamento de Física Aplicada, CINVESTAV-IPN, Mérida, Yuc. 97310, Mexico
Received: August 26, 2004; In Final Form: October 21, 2004

Dye-sensitized mesoporous nanocrystalline SnO_2 electrodes and the pseudohalogen redox mediator $(SeCN)_2$/$SeCN^-$ or $(SCN)_2$/SCN^- or the halogen redox mediator I_3^-/I^- were implemented for regenerative solar cell studies. Adsorption isotherms of the sensitizers $Ru(deeb)(bpy)_2(PF_6)_2$, $Ru(deeb)_2(dpp)(PF_6)_2$, and $Ru(deeb)_2(bpz)(PF_6)_2$, where deeb is 4,4′-diethylester-2,2′-bipyridine, dpp is 2,3-dipyridyl pyrazine, and bpz is bipyrazine, binding to the SnO_2 surface were well described by the Langmuir model from which the saturation coverage, $\Gamma_0 = 1.7 \times 10^{-8}$ mol/cm^2, and surface-adduct formation constant, $K_{ad} = 2 \times 10^5$ M^{-1}, were obtained. Following excited-state interfacial electron transfer, the oxidized sensitizers were reduced by donors present in the acetonitrile electrolyte as shown by transient absorption spectroscopy. With iodide as the donor, a rate constant $k > 10^8$ s^{-1} was measured for sensitizer regeneration. In regenerative solar cells, it was found that the incident photon-to-current conversion efficiencies and open circuit voltages (V_{oc}) were comparable for $(SeCN)_2$/$SeCN^-$ and I_3^-/I^- for all three sensitizers. The V_{oc} varied linearly with the logarithm of the short circuit photocurrent densities (J_{sc}), with typical correlations of ∼50−60 mV/decade. Capacitance measurements of the SnO_2 electrode in the presence of I_3^-/I^-, $(SeCN)_2$/$SeCN^-$, or $(SCN)_2$/SCN^- are reported.

Introduction

Efficient conversion of sunlight to electrical power is an important goal.[1] Sensitized nanocrystalline (anatase) TiO_2 thin films have renewed interest in molecular approaches to this objective.[2a−c] Regenerative photoelectrochemical cells based on these materials with an organic electrolyte based on the triiodide/iodide, I_3^-/I^-, redox mediators have yielded global conversion efficiencies of 10.6% under simulated AM 1.5 solar irradiance conditions.[3] It is often found that absorbed photons are converted to electrons near quantitatively, while only a small fraction of the free energy stored in the sensitizer excited state contributes to open circuit photovoltage (V_{oc}).[2] In other words, the kinetics of the dye-sensitized solar cells appears to be well optimized while the thermodynamics is not.

A significant fraction of the wasted free energy in these cells can be attributed to the use of one redox mediator, I_3^-/I^-, regardless of the molecular sensitizer. Ideally, a redox mediator should be optimized for each particular molecular sensitizer used within the cell. Alternative redox mediators, such as quinone/hydroquinone,[4] Br_2/Br^-,[4] Fc^+/Fc (where Fc is ferrocene),[5] PTZ^+/PTZ (where PTZ is phenothiazine),[6] and solid-state hole conductors,[7a−b] have been far less effective for energy conversion. Recent reports of cobalt-based mediators are particularly encouraging but thus far compare well to I_3^-/I^- only at irradiances below one sun.[8] Very recently, a high 7.5% efficiency solar cell was reported based on the $(SeCN)_3^-$/$SeCN^-$ redox mediator in solvent-free ionic liquid electrolyte.[9]

We previously reported on the use of the pseudohalide redox mediators $(SeCN)_2$/$SeCN^-$ and $(SCN)_2$/SCN^- in dye-sensitized TiO_2 (anatase) solar cells in acetonitrile.[9] With *cis*-$Ru^{II}(dcbH_2)_2(NCS)_2$, where $dcbH_2$ is 4,4′-$(CO_2H)_2$-2,2′-bipyridine, as the sensitizer, low photocurrent efficiencies were observed. Despite having more positive formal reduction potentials than that of I_3^-/I^-, only a slight increase in V_{oc} was measured using $(SeCN)_2$/$SeCN^-$, and the cell potential obtained using $(SCN)_2$/SCN^- was considerably worse. Transient spectroscopic studies revealed that the excited-state electron injection yields were high and independent of the redox mediator employed. However, sluggish oxidation rates of the pseudohalides by *cis*-$Ru^{III}(dcbH_2)_2(NCS)_2^+$ allowed a significant fraction of the injected electrons to recombine with the oxidized sensitizer thereby decreasing the solar conversion efficiency.

Ruthenium sensitizers based on bipyrazine (bpz) and 2,3-dipyridyl pyrazine (dpp) ligands with $Ru^{III/II}$ reduction potentials that are ∼550−900 mV more positive than that of *cis*-$Ru^{II}(dcbH_2)_2(NCS)_2$ were independently prepared and tested, Scheme 1.[10] While these sensitizers absorb light less efficiently in the red region, the hope was that the increase in V_{oc} would compensate for this and higher power conversion yields would be realized. However, these photoexcited sensitizers did not inject electrons into TiO_2 with high quantum yields. In some cases, even the reduced sensitizers, i.e., $Ru(dcbH_2)(bpz^-)(bpz)^+$, did not transfer electrons to TiO_2 effectively, indicating that neither the excited or the reduced state was a sufficiently strong reducing agent to inject electrons into the TiO_2 conduction band.[10]

In the present work, we have turned to nanocrystalline SnO_2 thin films. The conduction band-edge of single-crystal SnO_2 is reported to be ∼500 mV more positive than that of single-crystal rutile TiO_2 in aqueous electrolytes.[11] There exists experimental evidence that this is also true for the nanocrystalline SnO_2.[12] Even though the aqueous conduction band-edge given in Scheme 1 indicates unfavorable thermodynamics for injection from $Ru(deeb)_2(dpp)^{2+}$* and $Ru(deeb)_2(bpz)^{2+}$*, we emphasize that injection may occur from "hot" excited states and that the "acceptor states" relevant to nanocrystalline metal oxides may have an exponential density of unfilled states rather than the abrupt edge indicated in Scheme 1.[2] Therefore, our expectation

* To whom correspondence should be addressed.
[†] The Johns Hopkins University.
[‡] CINVESTAV-IPN.

10.1021/jp0461347 CCC: $30.25
Published on Web 12/21/2004

SCHEME 1: Conduction Band-Edge Energy of Single Crystal SnO_2 (E_{CB} at pH = 1) with the Ground- and Excited-State Reduction Potentials of the Ruthenium Sensitizers and the Reduction Potentials of the Mediators in Acetonitrile[a]

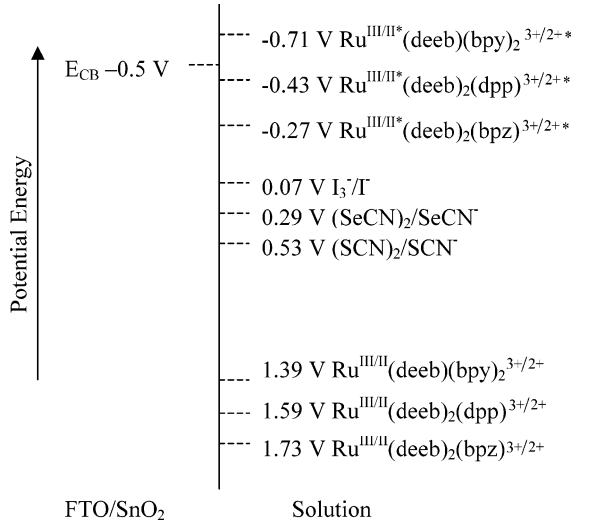

[a] All potentials are vs SCE.

was that $Ru(deeb)_2(dpp)^{2+*}$ and $Ru(deeb)_2(bpz)^{2+*}$ would inject electrons into SnO_2 more effectively than into TiO_2. The positive $Ru^{III/II}$ potentials should also result in more rapid oxidation of the pseudohalides and iodide and produce higher photocurrent efficiencies. These expectations were in fact realized. Furthermore, we discovered conditions where regenerative solar cells with the pseudohalides yielded comparable and even slightly higher photocurrents and open circuit photovoltages than did iodide. We also report evidence for static ($k > 10^8\ s^{-1}$) oxidation of iodide within dye-sensitized solar cells.

Experimental Section

Materials. The sensitizers $Ru(deeb)(bpy)_2(PF_6)_2$, $Ru(deeb)_2(dpp)(PF_6)_2$, and $Ru(deeb)_2(bpz)(PF_6)_2$ were available from previous studies.[10] Reagents were obtained as follows: CH_3CN (Burdick and Jackson, BioSyn grade); $Pb(SCN)_2$ (Aldrich, 99.5%); Br_2 (Aldrich, 99.5%); NaI (Aldrich, 99.5%); I_2 (Aldrich, 99.8%); NaSCN (Alfa Aesar, 98%); KSeCN (Alfa Aesar, 98.5%); $LiClO_4$ (Aldrich, 99.99%); poly(ethylene glycol) reacted with bisphenol A diglycidyl ether (Aldrich, $M_n \sim 15\,000$); $NaHCO_3$ (EM Science, 99.7%); NaOH (EM Science, 97%); microscope slides (VWR); and fluorine-doped tin oxide (FTO) (Pilkington, 7 Ω/square). Commercially available SnO_2 as a 15% aqueous colloidal solution of 15 nm particles was used as received from Alfa Aesar.

SnO_2 Thin Film Preparation. Poly(ethylene glycol), 0.6 g, and 0.5 mL of a pH 11 $NaHCO_{3(aq)}/NaOH_{(aq)}$ solution were combined and dissolved with 10 mL of colloidal $SnO_{2(aq)}$ and stirred for ∼2 h. This solution was applied to an FTO or microscope slide with an adhesive tape mask and spin coated at 2000 rpm for 12 s using a Laurell Technologies Corp. WS-400A-6NPP/LITE spinner. The tape was removed after 30 min of air-drying, and the films were heated at 450 °C for 30 min under a slow flow of oxygen. The ruthenium compounds were attached to SnO_2 by surface reactions in acetonitrile solutions containing ∼100 mM sensitizer for 24 h.

Absorbance. Steady-state absorption measurements were made on a Hewlett-Packard 8453 diode array spectrophotometer. Transient absorption spectra were acquired as previously described.[13]

Photoluminescence. Steady-state photoluminescence (SSPL) spectra were obtained with a Spex Fluorolog that had been calibrated with a NIST standard tungsten−halogen lamp.[14] Time-resolved measurements were obtained as previously described.[14]

Solar Cell Electrolyte. The electrolyte solutions were freshly prepared immediately before each set of experiments as previously described.[10]

Photoelectrochemistry. The photoanode consisted of colloidal SnO_2 deposited upon an FTO substrate sensitized with either $Ru(deeb)(bpy)_2(PF_6)_2$, $Ru(deeb)_2(dpp)(PF_6)_2$, or $Ru(deeb)_2(bpz)(PF_6)_2$. The counter electrode consisted of an FTO substrate with a thin Pt coating. Measurements were performed in a two-electrode cell at room temperature using the I_3^-/I^- redox mediator, and at 0 °C for the $(SeCN)_2/SeCN^-$ and $(SCN)_2/SCN^-$ redox mediators, with preparations discussed elsewhere.[10] A 150 W Xe lamp coupled to a *f*/2 0.2 m McPherson monochromator was used for incident photon-to-current efficiency (IPCE) measurements. The 488 nm laser line of an Innova argon ion laser was used as the excitation source for photocurrent density vs photovoltage and for irradiance-dependent measurements. Plasma lines were removed using a 488 nm notch filter, and the flux was attenuated using a beam collimator. Incident irradiances were measured using an S370 UDT optometer. Photocurrents and photovoltages were obtained using a Keithley 617 electrometer and a Keithley 199 System DMM/Scanner, respectively.

Impedance Spectroscopy. Impedance and capacitance of FTO/SnO_2 samples were measured using a Stanford Research SR530 lock-in amplifier (LIA) and a PAR model 173 potentiostat/galvanostat. All measurements were done in a three-electrode configuration using a Pt gauze counter electrode, a 10 mM $AgNO_3$/Ag reference electrode in acetonitrile, and an FTO/SnO_2 sample as the working electrode. The geometry of the electrochemical cell was the same throughout the experiments, enforcing a minimal distance between electrodes and a 0.28 cm^2 working electrode area.

Using a LabView program, the LIA and potentiostat were programmed to obtain frequency vs impedance scans and potential vs capacitance scans. The LIA was used to generate both the reference signal and the modulating signal (3 mV peak to peak) of known frequency. The modulating signal was added onto the potential generated by the potentiostat. The current to voltage output of the potentiostat was connected to the voltage input of the LIA. The LIA was then used to measure the real and imaginary part of the current in the electrochemical cell as a function of either frequency or potential. The real and imaginary current impedance (Z) and capacitance (C) were calculated by the program. Complex plane plots of the impedance ($|\mathrm{Im}(Z)|$ vs $\mathrm{Re}(Z)$), Bode plots ($\log(|Z|)$ vs $\log(\omega)$), and C vs potential plots were also produced by the LabView program.

Results

The trischelated ruthenium sensitizers $Ru(deeb)(bpy)_2(PF_6)_2$, $Ru(deeb)_2(dpp)(PF_6)_2$, and $Ru(deeb)_2(bpz)(PF_6)_2$ were anchored to nanocrystalline SnO_2 thin films. The metal-to-ligand charge-transfer (MLCT) absorption maximum ($\lambda_{max.abs}$) was observed at 475 nm in solution and blue shifted to 456 nm following surface attachment to SnO_2 (Figure 1). Steady-state photoluminescence from the excited sensitizer (S*) was observed with an emission maximum ($\lambda_{max.em}$) at 690 nm in solution, which blue shifted to 665 nm following surface attachment to SnO_2 (Figure 1).

Adsorption isotherms were measured and found to be consistent with the Langmuir model, eq 1.[15] The surface-adduct

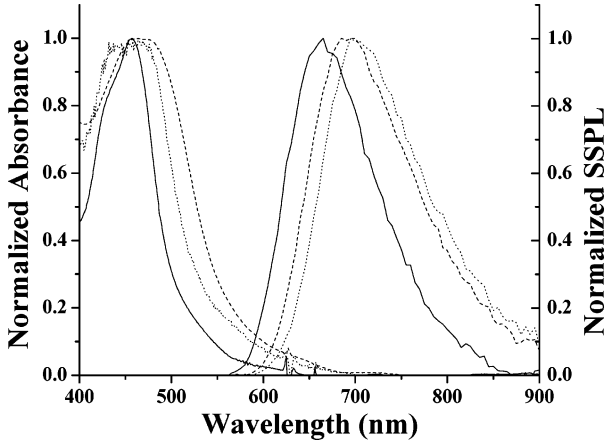

Figure 1. Normalized ground-state absorbance and steady-state photoluminescence vs wavelength of $Ru(deeb)(bpy)_2(PF_6)_2$ (solid line), $Ru(deeb)_2(dpp)(PF_6)_2$ (dashed line), and $Ru(deeb)_2(bpz)(PF_6)_2$ (dotted line) on SnO_2 in argon-purged acetonitrile solution.

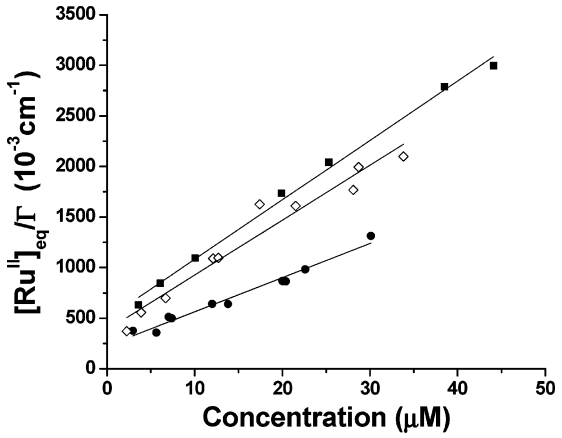

Figure 2. A Langmuir binding isotherm model of $Ru(deeb)(bpy)_2(PF_6)_2$ (squares), $Ru(deeb)_2(dpp)(PF_6)_2$ (circles), and $Ru(deeb)_2(bpz)(PF_6)_2$ (diamonds), applied to the SnO_2 surface. Absorbance values were recorded after 24 h of soaking.

TABLE 1: Ground-State Absorption Maxima $\lambda_{max.abs}$, Steady-State Photoluminescence Maxima $\lambda_{max.em}$, Surface Adduct Formation Constant K_{ad}, and Saturation Surface Coverages Γ_0

sensitizer	$\lambda_{max.abs}$ (nm)	$\lambda_{max.em}$ (nm)	K_{ad} (M^{-1})	Γ_0 (mol/cm^2)
$Ru(deeb)(bpy)_2^{2+}$	456	665	1.2×10^5	1.7×10^{-8}
$Ru(deeb)_2(dpp)^{2+}$	447	695	1.5×10^5	3.0×10^{-8}
$Ru(deeb)_2(bpz)^{2+}$	464	695	1.4×10^5	1.8×10^{-8}

formation constant, K_{ad}, and saturation coverage, Γ_0, were evaluated using ground-state absorption measurements. Here, Γ refers to the surface coverage, and $[Ru^{II}]_{eq}$ represents the solution concentration at equilibrium. After 24 h, complete equilibration was accomplished, and further soaking times were no longer required (Figure 2). For $Ru(deeb)(bpy)_2(PF_6)_2$, K_{ad} and Γ_0 were estimated to be 1.2×10^5 M^{-1} and 1.7×10^{-8} mol/cm^2, respectively. Table 1 summarizes these data for all three sensitizers.

$$\frac{[Ru^{II}]_{eq}}{\Gamma} = \frac{1}{K_{ad}\Gamma_0} + \frac{[Ru^{II}]_{eq}}{\Gamma_0} \qquad (1)$$

Excited-state reduction potentials, $E°$ ($Ru^{III/II}*$), of the sensitizers bound to SnO_2 were obtained using eq 2.[16] The free energy stored within the excited state, ΔG_{es}, was estimated by

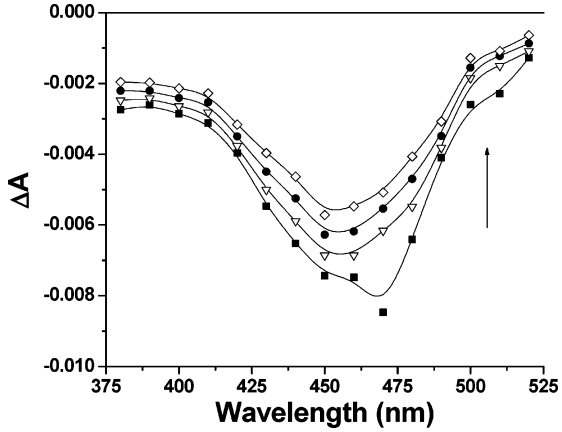

Figure 3. Transient absorbance difference spectra of $Ru(deeb)(bpy)_2/SnO_2$ in 0.25 M $LiClO_4$ measured at 0 ns (squares), 200 ns (upside down triangles), 500 ns (circles), and 1000 ns (diamonds) after pulsed 532 nm excitation (6.2 mJ/cm^2).

a tangent line drawn on the high-energy side of the corrected steady-state photoluminescence and was estimated to be 2.1 eV for $Ru(deeb)(bpy)_2*/SnO_2$. The formal $Ru^{III/II}$ reduction potentials in acetonitrile solution and anchored to metal oxide surfaces have previously been shown to be the same within ±20 mV.[10,14,17] Therefore, the solution reduction potentials were used as an estimate of the potentials for the surface-bound sensitizers.[10b] For $Ru(deeb)(bpy)_2/SnO_2$, the ground- and excited-state reduction potentials were 1.39 and −0.71 V vs saturated calomel electrode (SCE), respectively.

$$E°(Ru^{III/II}*) = E°(Ru^{III/II}) - \Delta G_{es} \qquad (2)$$

The transient absorption difference spectra of sensitized films in a 0.25 M $LiClO_4$ acetonitrile solution were obtained after pulsed 532 nm light excitation (Figure 3). The transient spectra were dominated by the presence of the oxidized sensitizer with some minor contributions from excited states observed at early times. Contributions from the excited state were significant in the transient absorption spectra observed after pulsed light excitation of $Ru(deeb)_2(bpz)/SnO_2$ and $Ru(deeb)_2(dpp)/SnO_2$, and the excited states decayed with nonexponential kinetics and half-lives of ∼10 and 30 ns, respectively.

The transient absorbance difference spectra of the sensitized films were acquired as a function of the electron donor present in the external surrounding 0.25 M $LiClO_4$ acetonitrile solution. The single wavelength data shown in Figure 4a correspond to recovery of the ground-state sensitizer in the absence of an electron donor. Data for Figure 4b−d were measured under identical experimental conditions except in the presence of 100 mM concentrations of SCN^-, $SeCN^-$, or I^-, respectively. There were negligible errors due to competitive absorption of the excitation beam by the reducing agents or their oxidized forms at this wavelength.[9] The transient absorbance difference spectra of $Ru(deeb)(bpy)_2/SnO_2$ as a function of I^- concentration in the surrounding 0.25 M $LiClO_4$ acetonitrile solution are shown in Figure 5. Absorption changes were monitored at 500 nm (Ru^{3+} absorption) and at 400 nm ($I_2^{\bullet-}$ absorption) for 0 mM, 1 mM, 10 mM, and 1 M I^- concentrations. The effect of iodide was found to be reversible by replacing the iodide solution with the 0.25 M $LiClO_4$ acetonitrile solution.

Capacitance data for the unsensitized tin oxide electrodes in acetonitrile solutions of I_3^-/I^-, $(SeCN)_2/SeCN^-$, or $(SCN)_2/SCN^-$ are shown in Figure 6. The graph shows significant capacitance increase at 25, −100, and 400 mV vs $Ag/AgNO_3$

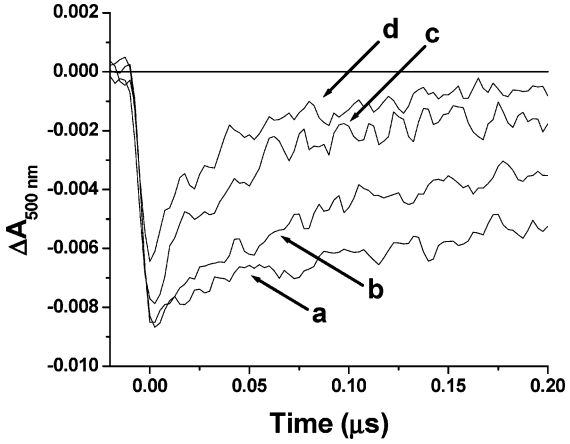

Figure 4. Transient absorbance kinetics monitored at 500 nm following pulsed 532 nm excitation of $Ru(deeb)_2(dpp)/SnO_2$ in 0.25 M $LiClO_4$ acetonitrile solutions with (a) no electron donor, (b) 100 mM NaSCN, (c) 100 mM KSeCN, and (d) 100 mM NaI.

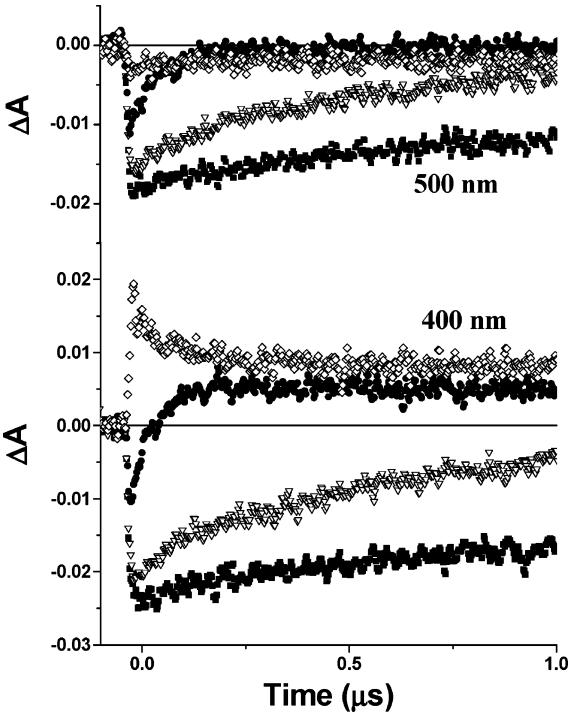

Figure 5. Transient absorbance changes monitored at 500 nm (upper) and 400 nm (lower) after pulsed 532 nm excitation (12 mJ/cm^2) of $Ru(deeb)(bpy)_2/SnO_2$ in argon-saturated, 0.25 M $LiClO_4$ acetonitrile with 0.00 mM (squares), 1 mM (upside down triangles), 10 mM (circles), and 1 M (diamonds) NaI.

for SnO_2 samples in electrolytes containing I_3^-/I^-, $(SeCN)_2/SeCN^-$, and $(SCN)_2/SCN^-$, respectively. Note that in this potential window the fluorine-doped tin oxide substrate (without colloidal SnO_2) showed no sharp changes in capacitance. The rise in capacitance is attributed to an increase in space charge and/or Helmholtz layer capacitance. The latter is expected to increase as the electrode surface area increases. Capacitance measurements of the FTO/SnO_2 electrode were also performed in 0.25 M $LiClO_4$ acetonitrile solution.

Photoelectrochemical measurements were obtained with $(SeCN)_2/SeCN^-$, I_3^-/I^-, or $(SCN)_2/SCN^-$ as redox mediators. IPCE values were recorded, and the relative efficiencies were $(SeCN)_2/SeCN^- > I_3^-/I^- > (SCN)_2/SCN^-$ for $Ru(deeb)(bpy)_2/SnO_2$ (Figure 7). The ground-state absorbance at 455 nm was

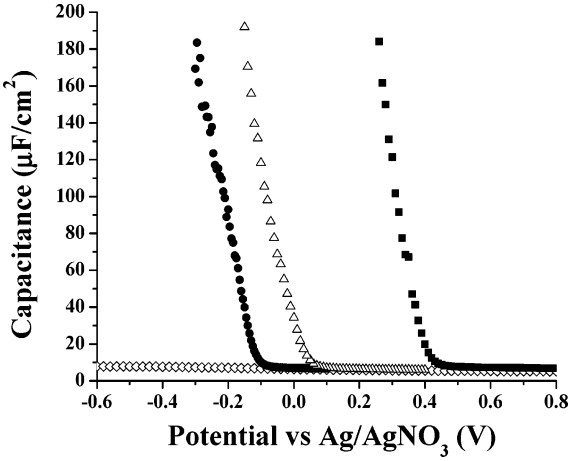

Figure 6. Capacitance vs potential plots for unsensitized FTO/SnO_2 measured at a 100 Hz frequency with a peak-to-peak voltage oscillation of 3 mV. The electrolytes used were 25/100 mM concentrations of $(SeCN)_2/SeCN^-$ (circles), I_3^-/I^- (triangles), and $(SCN)_2/SCN^-$ (squares), in 0.25 M $LiClO_4$ acetonitrile. Also shown are data for the FTO substrate (diamonds) in 0.25 M $LiClO_4$ acetonitrile electrolyte.

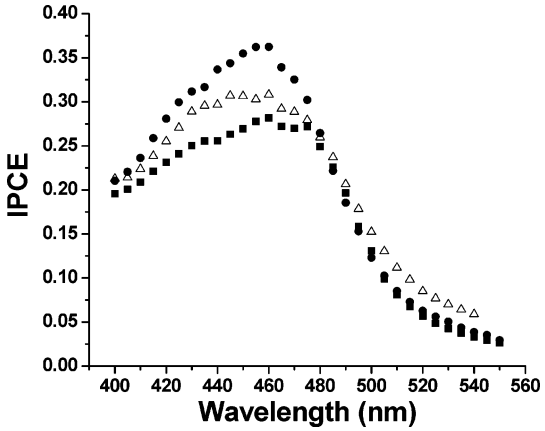

Figure 7. IPCEs versus wavelength of $Ru(deeb)(bpy)_2/SnO_2$ in 0.25 M $LiClO_4$ acetonitrile solutions with $(SeCN)_2/SeCN^-$ (circles), I_3^-/I^- (triangles), and $(SCN)_2/SCN^-$ (squares) redox mediators at 25 mM/100 mM concentrations.

TABLE 2: Absorbed Photon-to-Current Conversion Efficiencies Measured at the Absorption Maximum for Each Sensitizer with ~1 mW/cm^2 Irradiance

	redox mediator		
sensitizer	I_3^-/I^-	$(SeCN)_2/SeCN^-$	$(SCN)_2/SCN^-$
$Ru(deeb)(bpy)_2^{2+}$	0.56	0.65	0.51
$Ru(deeb)_2(dpp)^{2+}$	0.31	0.35	0.22
$Ru(deeb)_2(bpz)^{2+}$	0.15	0.29	0.33

TABLE 3: Open Circuit Voltage (V_{oc}) Measured at the Absorption Maximum for Each Sensitizer with ~1 mW/cm^2 Irradiance

	redox mediator		
sensitizer	I_3^-/I^-	$(SeCN)_2/SeCN^-$	$(SCN)_2/SCN^-$
$Ru(deeb)(bpy)_2^{2+}$	282	330	84
$Ru(deeb)_2(dpp)^{2+}$	253	286	150
$Ru(deeb)_2(bpz)^{2+}$	258	297	115

~0.35 for all samples, indicating a light harvesting efficiency (LHE) of 0.55. The absorbed photon-to-current conversion efficiencies (APCEs) and open circuit voltages (V_{oc}) at λ_{max} for all combinations of sensitizers and redox mediators are summarized in Table 2 and Table 3, respectively. Photocurrent densities (J_{pc}) vs photovoltage (V) measurements were obtained

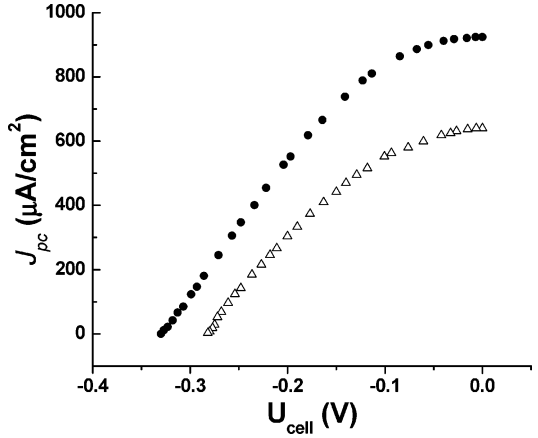

Figure 8. Photocurrent density (J_{pc}) vs photovoltage curves of Ru(deeb)(bpy)$_2$/SnO_2 in 0.25 M $LiClO_4$ acetonitrile solutions with $(SeCN)_2$/$SeCN^-$ (circles) and I_3^-/I^- (triangles) as redox mediators at 25 mM/100 mM concentrations. Approximately 11.1 mW/cm^2 of monochromatic 488 nm illumination was used.

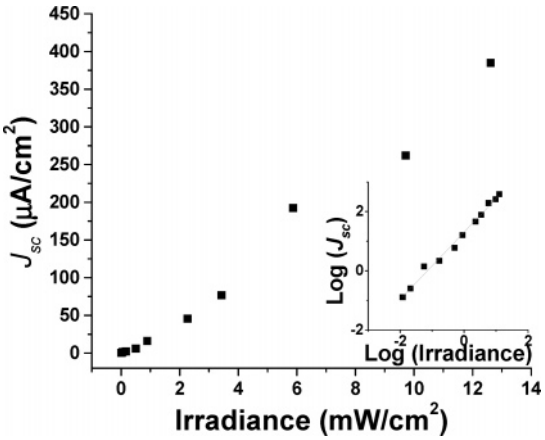

Figure 9. Short circuit photocurrent density (J_{sc}) vs 488 nm irradiance for Ru(deeb)(bpy)$_2$/SnO_2 in 0.25 M $LiClO_4$ acetonitrile solution with $(SeCN)_2$/$SeCN^-$ as the redox mediator at 25 mM/100 mM concentration. The inset shows the log(J_{sc}) vs log(irradiance).

TABLE 4: Short Circuit Photocurrent Densities (J_{sc}), Open Circuit Voltages (V_{oc}), and Fill Factors Obtained under ~11.1 mW/cm^2 of 488 nm Illumination Using $(SeCN)_2$/$SeCN^-$ as the Redox Mediator[a]

sensitizer	J_{sc} (μA/cm^2)	V_{oc} (mV)	fill factor
Ru(deeb)(bpy)$_2^{2+}$	923	330	0.36
Ru(deeb)$_2$(dpp)$^{2+}$	454	286	0.39
Ru(deeb)$_2$(bpz)$^{2+}$	423	297	0.38

[a] The ground-state absorbance was ~0.2 at 488 nm.

using 11.1 mW/cm^2 of 488 nm light, and the relative efficiencies were $(SeCN)_2$/$SeCN^-$ > I_3^-/I^- > $(SCN)_2$/SCN^- for Ru(deeb)(bpy)$_2$/SnO_2 (Figure 8). The ground-state absorbance at 488 nm was ~0.20 for all samples, implying an absorptance (or light harvesting efficiency) of 0.37. Table 4 summarizes the short circuit photocurrent densities J_{sc}, open circuit photovoltage V_{oc}, and fill factors (ff's) using the $(SeCN)_2$/$SeCN^-$ redox mediator with each sensitizer. Photocurrents and photovoltages obtained with $(SCN)_2$/SCN^- were low in part because of some degradation observed during the $I-V$ measurement, suggesting that this redox mediator lacks practical utility at room temperature. J_{sc} varied linearly with low irradiances and began to saturate at higher photon fluxes for all combinations of redox mediators and sensitizers (Figure 9). The logarithm of J_{sc} varied linearly with the logarithm of irradiance, with correlations ranging from ~0.8 to 1.1 (Table 5). V_{oc} varied linearly with the logarithm of the J_{sc}, with typical correlations of ~50−60 mV/decade J_{sc} (Figure 10 and Table 5).

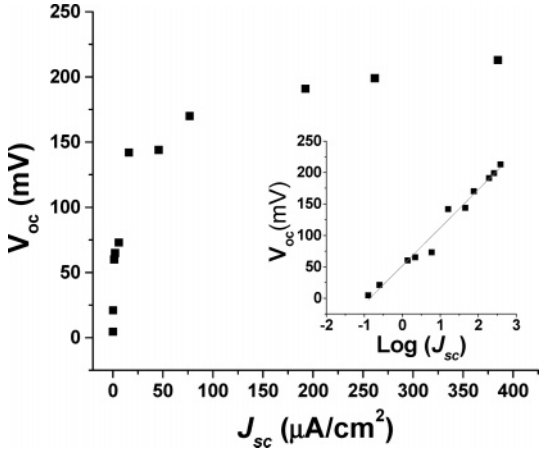

Figure 10. Open circuit photovoltage (V_{oc}) vs short circuit photocurrent density (J_{sc}) at different 488 nm irradiances of Ru(deeb)(bpy)$_2$/SnO_2 in 0.25 M $LiClO_4$ acetonitrile solution and $(SeCN)_2$/$SeCN^-$ as the redox mediator at 25 mM/100 mM concentration. The inset shows a plot of open circuit photovoltage vs log(J_{sc}) with a superimposed best fit line.

TABLE 5: The log(J_{sc}) Divided by the log(irradiance), and V_{oc} Divided by log(J_{sc})[a]

sensitizer	log(J_{sc})/log(irradiance)	V_{oc}/log(J_{sc}) (mV/decade)
Ru(deeb)(bpy)$_2^{2+}$	1.13	61
Ru(deeb)$_2$(dpp)$^{2+}$	0.94	58
Ru(deeb)$_2$(bpz)$^{2+}$	0.89	61

[a] Irradiance measurements were performed with 488 nm illumination and $(SeCN)_2$/$SeCN^-$ as the redox mediator.

Discussion

As stated in the Introduction, the goal of this study was to utilize ruthenium sensitizers with positive $Ru^{III/II}$ potentials for efficient light-to-electrical energy conversion using pseudohalide donors. It was found that Ru(II) sensitizers with bpz and dpp ligands were weak excited-state reductants, necessitating the use of nanocrystalline SnO_2 thin films rather than TiO_2. In this work, we have quantified the photophysical behavior of the surface-bound sensitizers and the performance of the sensitized materials in dye-sensitized solar cells under visible light illumination with $(SeCN)_2$/$SeCN^-$, $(SCN)_2$/SCN^-, and I_3^-/I^-.

Photophysical Behavior. The spectral sensitivity of SnO_2 was extended into the visible region following surface attachment of the sensitizers. Adsorption isotherms indicated that the surface-adduct formation constants, K_{eq}, with SnO_2 are comparable to those obtained on TiO_2 and ZrO_2 surfaces, ~10^5 M^{-1}.[14,18] The strong sensitizer−tin oxide adducts formed allowed us to quantify the excited-state behavior of the sensitized thin films in acetonitrile electrolyte without significant desorption.

The Ru(II) sensitizers possess MLCT excited states. The Ru → diimine ligand absorption bands overlap for these sensitizers. The nature of the MLCT excited state is most easily characterized by the sensitizers' time-resolved absorption and photoluminescence properties. Previous studies have clearly shown that the photoluminescent excited state has an electron localized on the most easily reduced ligand.[10] The reduction potentials become increasingly negative in the order: bpz < dpp < deeb < bpy. The observed shifts in the absorption and photoluminescence spectra upon surface binding can be understood based on this trend and the strong interaction between SnO_2 and the

deeb ligand. For example, the blue shifts observed upon surface attachment of Ru(deeb)$(bpy)_2^{2+}$ can be explained by destabilization of the excited state by the semiconductor nanoparticle. This same destabilization occurs for both Ru$(deeb)_2(dpp)^{2+}$ and Ru$(deeb)_2(bpz)^{2+}$; however for these sensitizers the excited state is localized on the "remote" dpp or bpz ligands and the photoluminescence spectrum is less sensitive to it. The small red spectral shifts observed for these sensitizers upon surface attachment can be rationalized by an inductive effect wherein the $Ru^{III/II}$ potentials become more negative upon surface binding. These spectral shifts are consistent with corresponding data for these sensitizers attached to TiO_2 and ZrO_2 indicating that these metal oxides perturb the MLCT excited state in a similar manner.[10]

Following photoexcitation of the sensitized materials in 0.25 M $LiClO_4$ acetonitrile solutions, both the excited state, Ru*/SnO_2, and charge separated state $Ru^{3+}/SnO_2(e^-)$ were present, except in the case of Ru(deeb)$(bpy)_2/SnO_2$ where only the charge separated state was observed. The lower electron injection yields and intense photoluminescence from Ru$(deeb)_2(dpp)/SnO_2$ and Ru$(deeb)_2(bpz)/SnO_2$ can be rationalized by the fact that they are much weaker excited-state reductants than is Ru(deeb)$(bpy)_2/SnO_2$.[21] Furthermore, for these compounds the thermally equilibrated excited state is localized on the dpp or bpz ligands that are not directly bonded to the SnO_2 surface.[10] This too could lower the electron injection yields and explains the lower photocurrent efficiency of the bpz and dpp compounds. While recombination of the injected electron with the oxidized sensitizer was not studied in detail, it was found that the process required milliseconds to complete, which is roughly consistent with behavior on TiO_2.

Sensitizer Regeneration. We have characterized the mechanisms for sensitizer regeneration (and hence donor oxidation) with nanosecond transient absorption spectroscopy. In this approach, a laser pulse is used to create the excited state and initiate electron transfer. Since injection almost always occurs on a subnanosecond time scale, the first product observed under our experimental conditions is the oxidized sensitizer and the injected electron. If an electron donor is present, the subsequent thermal electron-transfer reactions that regenerate the sensitizer ground state can be quantified. In previous studies of this type with *cis*-$Ru^{II}(dcb)_2(NCS)_2/TiO_2$, it was found that the excited-state interfacial electron-transfer yield was near unity and was independent of the I^-, $SeCN^-$, or SCN^- concentration. Reduction of *cis*-$Ru^{III}(dcb)_2(NCS)_2^+$ by I^- occurred within the first 100 ns, whereas $SeCN^-$ required microseconds. The oxidation of SCN^- could not compete kinetically with charge recombination, a trend consistent with slower rate constants at lower driving forces. The trend also correlated well with the measured photocurrent efficiencies.[10]

When these same experiments were repeated with the heteroleptic Ru(II) sensitizers on tin oxide, the amplitude of the transient absorption signals as well as the rates changed in the order $SCN^- > SeCN^- > I^-$. The amplitude change could be a result of decreased injection yield or of rapid nanosecond regeneration of the ground-state sensitizer. We believe it is only due to the latter and have compelling evidence for this with Ru(deeb)$(bpy)_2/SnO_2$. The decreased amplitude of the MLCT bleach after excitation of Ru(deeb)$(bpy)_2/SnO_2$ in the presence of iodide coincided with an immediate appearance of absorption features characteristic of $I_2^{\bullet-}$. This is consistent with rapid ($k > 10^8\ s^{-1}$) iodide oxidation and not a decreased injection yield.[22] Iodide[23] and thiocyanate[23−27] ions are known to adsorb at metal oxide surfaces, thereby allowing static oxidation by Ru(III) without diffusional limitations. The subsequent $I + I^- \rightarrow I_2^-$ reaction must also occur within 10 ns. To our knowledge, the appearance of subnanosecond donor oxidation has not been previously reported at any sensitized metal oxide interface. We note that the situation is more complex for Ru$(deeb)_2(dpp)/SnO_2$ and Ru$(deeb)_2(bpz)/SnO_2$ because both the excited and charge separated states were observed transiently at short times, which complicates analysis. However, the amplitude changes were qualitatively the same, suggesting that the rapid iodide oxidation also occurred for these sensitizers.

Electrochemistry and Photoelectrochemistry. Capacitance measurements on the unsensitized SnO_2 electrodes show a clear change in interfacial capacitance in the presence of the different redox mediators. In the dark under equilibrium conditions, the Fermi energy of the FTO electrode is expected to be equal to the redox potential in solution. When a more negative potential is applied, providing the FTO/SnO_2 contact is ohmic, electrons can flow from the FTO to the SnO_2 film and be transferred to the electron acceptor in solution. This is coupled with a large increase in the total capacitance as the entire SnO_2 surface area is accessible. At potentials more positive, the SnO_2 film is depleted, and mainly the FTO impedance is measured. As a consequence, the capacitance is expected to increase close to the redox potential in the solution and capacitance−voltage data should track the formal reduction potentials. Experimentally, we find that the capacitance data for $SeCN^-$ and I^- are reversed from this expectation. At this time, we do not have a clear explanation for why. Clearly, the interrelation of the energetics and kinetics results in a more complex system than described by our simplistic interpretation.

Solar cells comprised of nanocrystalline SnO_2 sensitized with Ru(deeb)$(bpy)_2(PF_6)_2$, Ru$(deeb)_2(dpp)(PF_6)_2$, or Ru$(deeb)_2(bpz)(PF_6)_2$ and a redox mediator based upon $(SeCN)_2/SeCN^-$, $(SCN)_2/SCN^-$, or I_3^-/I^- were studied for light-to-electrical conversion applications. SnO_2 electrodes sensitized with Ru(deeb)$(bpy)_2^{2+}$ exhibited the highest overall conversion efficiency. An APCE of ~0.85 is estimated using $(SeCN)_2/SeCN^-$, after taking into account transmission and competitive light absorption losses. These yields were greater than or equal to those obtained with I_3^-/I^-. We note that while the photocurrent increased linearly with irradiance, saturation was observed at higher photon fluxes. The fill factors were typically between 0.4 and 0.5 and are consistent with other reports for nanocrystalline SnO_2.[12a]

The relationship between open circuit voltage and incident irradiance within dye-sensitized solar cells comprised of n-type nanocrystalline semiconductors has been previously explored.[30] The small particle size limits band bending, and charge separation efficiencies rely upon the relative kinetic rate constants.[29] Equation 3 has previously been applied to dye-sensitized electrodes.[6,31−33] Here, the logarithmic term includes the flux of electrons into the semiconductor, I_{inj}, divided by the product of the charge recombination rate of injected electrons with acceptors, $k_i[A]_i$. Assuming the recombination rate constants and injection yields are irradiance independent, this equation predicts a 59 mV increase in V_{oc} for each decade of increased irradiance.

$$V_{oc} = \left(\frac{kT}{e}\right) \ln\left(\frac{I_{inj}}{n\sum k_i[A]_i}\right) \qquad (3)$$

The V_{oc} was found to logarithmically depend on the incident irradiance with a slope of 50−61 mV change in photovoltage per decade irradiance for all redox mediators at sensitized tin

oxide electrodes. Previous studies with SnO_2,[34] CdSe,[35] and ZnO[11] nanocrystalline semiconductor thin films are also in accordance with an exponential relationship between the irradiance and the V_{oc}. The slopes reported in the literature vary widely, and this may indicate a change in the recombination mechanism.

Conclusion

We have demonstrated that alternative redox mediators can be successfully used within dye-sensitized solar cells comprised of a nanocrystalline SnO_2 electrode. This observation is particularly exciting, since most studies to date have been limited to the use of I_3^-/I^-, thereby also restricting the types of sensitizers and semiconductors employed. Photocurrent efficiencies and cell voltages were larger using the alternative redox mediator $(SeCN)_2/SeCN^-$ compared to I_3^-/I^- for all three sensitizers. The photocurrents were linear with irradiances over 2−4 decades. A logarithmic dependence of V_{oc} with the incident irradiance was measured. We emphasize that while the solar-to-electrical energy conversion efficiencies reported here for these pseudohalide redox mediators and sensitized tin oxide represent a significant improvement,[10] they are still far behind the state-of-the-art regenerative solar cells based upon sensitized TiO_2 with I_3^-/I^- in organic solvents.[1]

Acknowledgment. We are grateful to the Division of Chemical Sciences, Office of Basic Energy Sciences, Office of Energy Research, U.S. Department of Energy, for grant support (DE-FG02-96ER14662).

References and Notes

(1) O'Regan, B.; Grätzel, M. *Nature* **1991**, *353*, 737−739.

(2) (a) Grätzel, M.; Moser, J. E. Solar Energy Conversion. In *Electron Transfer in Chemistry*; Balzani, V., Gould, I. R., Eds.; Wiley-VCH: Weinheim, Germany, 2001; Vol. V., pp 589−644. (b) Bergeron, B. V.; Meyer, G. J. New Approaches for Energy Conversion at Dye Sensitized Electrodes. In *Photovoltaics for the 21st Century I*; McConnell, R. D., Kapur, V. K., Eds.; The Electrochemical Society: Pennington, NJ, 2001; pp 173−183. (c) Hagfeldt, A.; Grätzel, M. *Acc. Chem. Res.* **2000**, *33*, 269−277.

(3) Grätzel, M. *J. Photochem. Photobiol. C* **2003**, *4*, 145.

(4) Vlachopoulos, N.; Liska, P.; Augustynski, J.; Grätzel, M. *J. Am. Chem. Soc.* **1988**, *110*, 1216−1220.

(5) Gregg, B. A.; Pichot, F.; Ferrere, S.; Fields, C. L. *J. Phys. Chem. B* **2001**, *105* (7), 1422−1429.

(6) Argazzi, R.; Bignozzi, C. A.; Heimer, T. A.; Castellano, F. N.; Meyer, G. J. *J. Phys. Chem. B* **1997**, *101* (14), 2591−2597.

(7) (a) Stathatos, E.; Lianos, P.; Zakeeruddin, S. M.; Liska, P.; Grätzel, M. *Chem. Mater.* **2003**, *15* (9), 1825−1829. (b) O'Regan, B.; Lenzmann, F.; Muis, R.; Wienke, J. *Chem. Mater.* **2002**, *14* (12), 5023−5029.

(8) Nusbaumer, H.; Moser, J.-E.; Zakeeruddin, S. M.; Nazeeruddin, M. K.; Grätzel, M. *J. Phys. Chem. B* **2001**, *105* (43), 10461−10464.

(9) Wang, P.; Zakeeruddin, S. M.; Moser, J.-E.; Humphry-Baker, R.; Grätzel, M. *J. Am. Chem. Soc.* **2004**, *126*, 7164−7165.

(10) (a) Oskam, G.; Bergeron, B. V.; Meyer, G. J.; Searson, P. C. *J. Phys. Chem. B* **2001**, *105* (29), 6867−6873. (b) Bergeron, B. V.; Meyer, G. J. *J. Phys. Chem. B* **2003**, *107* (1), 245−254.

(11) (a) Bedja, I.; Hotchandani, S.; Kamat, P. V. *J. Phys. Chem.* **1994**, *98* (15), 4133−4140. (b) Nozik, A. J.; Memming, R. *J. Phys. Chem.* **1994**, *100*, 13061−13078.

(12) Nasr, C.; Kamat, P. V.; Hotchandani, S. *J. Phys. Chem. B* **1998**, *102* (49), 10047−10056.

(13) Bergeron, B. V.; Kelly, C. A.; Meyer, G. J. *Langmuir* **2003**, *19* (20), 8389−8394.

(14) Galoppini, E.; Guo, W.; Zhang, W.; Hoertz, P. G.; Qu, P.; Meyer, G. J. *J. Am. Chem. Soc.* **2002**, *124* (26), 7801−7811.

(15) Langmuir, I. *J. Am. Chem. Soc.* **1918**, *40* (9), 1361−1403.

(16) (a) Arnold, D. R.; Baird, N. C.; Bolton, J. R.; Brand, J. C. D.; Jacobs, P. W. M.; DeMayo, P.; Ware, W. R. *Photochemistry. An Introduction*; Academic Press: New York, 1974; p 13. (b) Rehm, D.; Weller, A. *Isr. J. Chem.* **1970**, *8* (2), 259−267.

(17) Heimer, T. A.; D'Arcangelis, S. T.; Farzad, F.; Stipkala, J. M.; Meyer, G. J. *Inorg. Chem.* **1996**, *35* (18), 5319−5324.

(18) Farzad, F.; Thompson, D. W.; Kelly, C. A.; Meyer, G. J. *J. Am. Chem. Soc.* **1999**, *121* (23), 5577−5578.

(19) Benko, G.; Kallioinen, J.; Korppi-Tommola, J. E. I.; Yartsev, A. P.; Sundstrom, V. *J. Am. Chem. Soc.* **2002**, *124* (3), 489−493.

(20) Benko, G.; Myllyperkio, P.; Pan, J.; Yartsev, A. P.; Sundstrom, V. *J. Am. Chem. Soc.* **2003**, *125* (5), 1118−1119.

(21) Spitler, M. T.; Sonntag, L. P. *J. Phys. Chem.* **1985**, *89* (8), 1453−1457.

(22) Nasr, C.; Hotchandani, S.; Kamat, P. *Phys. Chem. B* **1998**, *102* (25), 4944−4951.

(23) Ferry, J. L.; Fox, M. A. *Langmuir* **1998**, *14* (7), 1725−1727.

(24) Kamat, P. *Langmuir* **1985**, *1* (5), 608−611.

(25) Draper, R. B.; Fox, M. A. *J. Phys. Chem.* **1990**, *94* (11), 4628−4634.

(26) Dogliotti, L.; Hayon, E. *J. Phys. Chem.* **1968**, *72* (5), 1800−1807.

(27) Colombo, D. P., Jr.; Bowman, R. M. *J. Phys. Chem* **1996**, *100* (47), 18445−18449.

(28) Finklea, H. O. *Semiconductor Electrodes*; Finklea, H. O., Ed.; Studies in Physical and Theoretical Chemistry, Vol. 55; Elsevier: Amsterdam, 1988; Chapter 1, pp 27−30.

(29) Albery, W. J.; Bartlett, P. N. *J. Electrochem. Soc.* **1984**, *131* (2), 315−325.

(30) Huang, S. Y.; Schlichthorl, G.; Nozik, A. J.; Grätzel, M.; Frank, A. J. *J. Phys. Chem. B* **1997**, *101* (14), 2576−2582.

(31) Argazzi, R.; Bignozzi, C. A.; Heimer, T. A.; Castellano, F. N.; Meyer, G. J. *J. Am. Chem. Soc.* **1995**, *117* (47), 11815−11816.

(32) Grätzel, M.; Kalyanasundaram, K. *Curr. Sci.* **1994**, *66* (10), 706−714.

(33) Kumar, A.; Santangelo, P. G.; Lewis, N. S. *J. Phys. Chem.* **1992**, *96* (2), 834−842.

(34) Nasr, C.; Hotchandani, S.; Kamat, P. V.; Das, S.; Thomas, K. G.; George, M. V. *Langmuir* **1995**, *11* (5), 1777−1783.

(35) Liu, D.; Kamat, P. V. *J. Phys. Chem.* **1993**, *97*, 10769−10773.